

Unsupervised Video Anomaly Detection via Flow-based Generative Modeling on Appearance and Motion Latent Features

MyeongAh Cho, Taeoh Kim, and Sangyoun Lee

Yonsei University, Seoul, South Korea
maycho0305, kto, syleee@yonsei.ac.kr

Abstract

Surveillance video anomaly detection searches for anomalous events such as crimes or accidents among normal scenes. Since anomalous events occur rarely, there is a class imbalance problem between normal and abnormal data and it is impossible to collect all potential anomalous events, which makes the task challenging. Therefore, performing anomaly detection requires learning the patterns of normal scenes to detect unseen and undefined anomalies. Since abnormal scenes are distinguished from normal scenes by appearance or motion, lots of previous approaches have used an explicit pre-trained model such as optical flow for motion information, which makes the network complex and dependent on the pre-training. We propose an implicit two-path AutoEncoder (ITAE) that exploits the structure of a SlowFast network and focuses on spatial and temporal information through appearance (slow) and motion (fast) encoders, respectively. The two encoders and a single decoder learn normal appearance and behavior by reconstructing normal videos of the training set. Furthermore, with features from the two encoders, we suggest density estimation through flow-based generative models to learn the tractable likelihoods of appearance and motion features. Finally, we show the effectiveness of appearance and motion encoders and their distribution modeling through experiments in three benchmarks which result outperforms the state-of-the-art methods.

Introduction

Anomaly detection is a task that finds unusual, unseen, or undefined abnormal data among normal data and can be also called outlier detection. This is a practical task that is directly related to real-world problems such as surveillance anomaly detection, defect detection in factories, X-ray security systems, or diagnosis of medical problems (Pimentel et al. 2014). In addition, anomaly detection is even more important because it can replace inefficient human monitoring for anomalous events, which is time-consuming and laborious, with an automated system.

Anomaly detection in surveillance video task detects abnormal events such as traffic monitoring, accidents, and crime using the petabytes of normal videos from CCTVs that present in most places in our daily lives. However,

Copyright © 2021, Association for the Advancement of Artificial Intelligence (www.aaai.org). All rights reserved.

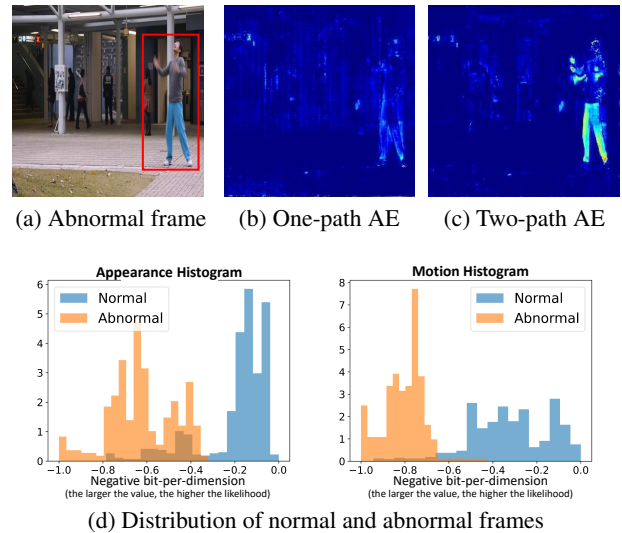


Figure 1: Reconstruction error of (b) one-path AE and the proposed (c) two-path AE at (a) abnormal input and (d) log-likelihood histogram (expressed in normalized negative bit-per-dimension) for its video clip. For a scene where a person throws a bag that the appearance factor is normal but the motion factor is abnormal, one-path AE reconstructs well, which fails to detect anomalies. One the other hand, two-path AE with appearance and motion path encoder shows high errors and each normality distribution of the encoder feature enables distinguishing of anomalies, especially in the motion distribution.

surveillance anomaly detection has several challenging issues. First, real-world anomalous events such as robberies and car accidents occur very infrequently compared to normal events, which brings a class imbalance problem between normal and abnormal data. Therefore, the training set of most surveillance anomaly detection databases only contains normal videos, and the anomalous event only exists in the test set. This makes it difficult to train in a general supervised manner that uses manually labeled data. Second, since anomalies are unbounded, it is impossible to define and collect all existing abnormal events, and labeling is ex-

tremely expensive. Therefore, detecting unseen and undefined anomalous events requires learning normality through abundant easily obtained normal videos.

Since the advent of deep learning, studies of surveillance anomaly detection task with a large amount of normal training dataset has grown significantly. Some studies (Zhu and Newsam 2019; Sultani, Chen, and Shah 2018) train classifiers through a supervised learning approach by consisting anomalies and their labels together in the training set. However, since supervised learning is dependent on anomalies in the training set, it is more suitable for specific abnormal class detection and solving general problems is difficult. Frame reconstruction or future prediction-based methods are mainly used as an unsupervised learning approach where the training set consists of only normal data without labeled anomalies (Hasan et al. 2016; Liu et al. 2018). AutoEncoder (Bengio et al. 2007) (AE)-structured networks that learn reconstruction (or prediction) tasks with just normal scenes cannot reconstruct properly when abnormal scenes are input during the testing time and this brings high errors between the input and output for anomaly detection. This approach enables training without labeled data and has made great progress.

Anomalous events in a surveillance system can be distinguished from normal events by appearance, motion, or both. For example, the passing of non-pedestrian objects such as cars on the sidewalk has a different appearance to a normal scene; fighting or loitering people show differences in motion; people throwing abnormal objects show differences in both. In other words, it is important to extract features that contain the appearance and motion of the input video for anomaly detection. Since temporal information is important in surveillance anomaly detection, many AE-based methods use explicit motion information with a pre-trained network such as optical flow networks (Nguyen and Meunier 2019a; Liu et al. 2018), pose estimator (Markovitz et al. 2020), or action recognition backbone (Zhong et al. 2019). However, this makes the network more complex and dependent on the pre-trained network. Inspired by the SlowFast Network (Feichtenhofer et al. 2019), which captures implicit motion and appearance features and brings satisfactory performance in action recognition tasks, we design an implicit two-path AE (ITAE) structure that encodes spatial and temporal representative features and decodes them together. Since it is difficult to simply contain motion information with an AE structure, the two encoders have different temporal and channel sizes to focus on appearance or motion information and a single decoder combines each feature for reconstruction. In Fig. 1, we visualized the output results of AE when the appearance of the input frame looks normal but the motion is abnormal. Compared with one-path AE, two-path AE shows a larger reconstruction error because the motion of the input frame is different from the learned normal frames.

When the reconstruction-based model capacity becomes too powerful and generalized, the error is lowered by the well reconstructed abnormal events (Schlegl et al. 2017) (shown in Fig. 1 (b)). To compensate for this drawback, we suggest the distribution learning of normal appearance and motion features extracted from AE by using a flow-based

generative model that estimates the density of input features. The flow-based model (Dinh, Krueger, and Bengio 2014) is a generative model that focuses on the density estimation of high-dimensional data with tractable exact log-likelihood. Therefore, by maximizing the likelihood of the flow-based generative model, it is possible to learn high-dimensional video features of appearance and motion normality. After training, abnormal events are found by out-of-distribution detection within input frames' feature likelihood (Shown in Fig. 1 (d)). To summarize the contributions of this paper,

- In anomaly detection in surveillance video task, it is important to learn the normal appearance and motion patterns. For representative spatio-temporal feature learning of normal video, inspired by the SlowFast network, we propose an implicit two-path AE in which appearance and motion features are captured along with two encoders where a decoder combines them for reconstruction without using any pre-trained network.
- To the best of our knowledge, we are the first to estimate the distribution of normal appearance and motion surveillance video features by utilizing a flow-based generative model.
- The proposed approach is in an unsupervised learning manner without pre-trained models or labeled data and shows superior performance on three surveillance anomaly detection benchmarks.

Related Works

Convolutional Networks for Video. As a basic network for video data, 3D convolution based networks have been proposed (Tran et al. 2015; Carreira and Zisserman 2017) and used for feature extraction in video anomaly detection. For video recognition, two-stream networks also have been proposed to model motion features explicitly (Christoph and Pinz 2016; Feichtenhofer, Pinz, and Zisserman 2016). However, these require the explicit extraction of temporal information using temporal differences or optical flows. Recently, SlowFast networks (Feichtenhofer et al. 2019) proposes two-path convolutional networks that implicitly extracts stationary and motion information. The slow-pathway extracts static appearance features using a narrow temporal window while the fast-pathway captures motion information using a higher temporal rate. The fusion of both exhibits promising results in video recognition using fewer parameters than conventional networks.

Video Anomaly Detection. Based on the powerful representation ability of deep convolutional networks, many anomaly detection algorithms based on frame reconstruction have been proposed. These algorithms exploit the structure of convolutional autoencoders (Hasan et al. 2016; Nguyen and Meunier 2019a), recurrent neural networks (Luo, Liu, and Gao 2017b,a), or 3D convolutions (Zhao et al. 2017). Other algorithms have been proposed via learning reconstruction with other objectives (Nguyen and Meunier 2019b), memory modules (Gong et al. 2019; Park, Noh, and Ham 2020), or reconstructing optical flows from frames (Ra-

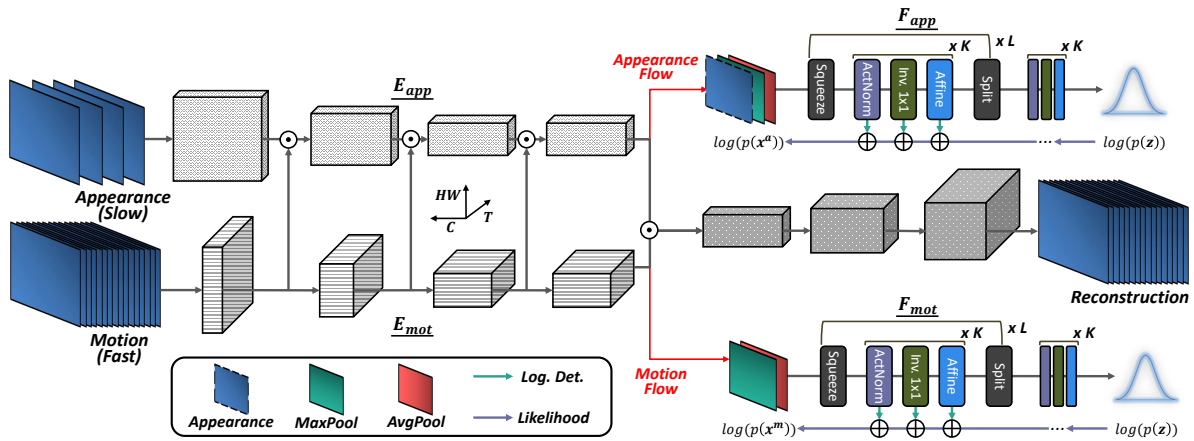


Figure 2: The overall framework of the proposed approach. Different frame rates are input into the appearance and motion encoders, which focus on spatial and temporal information, respectively. The latent features are concatenated and reconstructed into input frames by a single decoder. In addition, the max-pooling and average-pooling of each latent feature are concatenated and passed through the flow-based generative model to estimate the likelihood of normal appearance and motion features.

vanbaksh et al. 2017; Ganokratanaa, Aramvith, and Sebe 2020).

To increase the probability of unpredictability for abnormal samples, frame prediction-based approaches have been proposed (Liu et al. 2018; Lu et al. 2019). Some methods using bi-directional frame prediction have been proposed (Lee, Kim, and Ro 2018, 2019; Chen et al. 2020). However, prediction-based approaches generally require heavier structures or optical flows, and bi-directional models heavily rely on future frames.

As another category, anomaly detection methods via consisting and learning the compactness of normal clusters have been proposed. Clusters are configured by removing the most discriminant features (Tudor Ionescu et al. 2017), removing small clusters of normal samples (Ionescu et al. 2019b), features from the reconstruction objective (Xu et al. 2017) or extracting from a pre-trained object detector (Ionescu et al. 2019a) or pose estimator (Markovitz et al. 2020).

Generative Models. Compared to discriminative models, generative models do not require either normal annotations or proxy tasks such as frame generation. Some approaches based on a Gaussian model (Sabokrou et al. 2017, 2018a) or non-parametric density estimation (Hinami, Mei, and Satoh 2017) have been proposed based on either latent features or extracted features.

Deep generative models can be categorized into implicit and explicit density estimation models (Goodfellow 2016). However, implicit density models such as GANs (Goodfellow et al. 2014) do not define the data likelihood and cannot be used the in-distribution estimation without modifying the discriminator for the likelihood estimator (Sabokrou et al. 2018b), while explicit models first define likelihoods and try to maximize the likelihoods. An approximation-based model has been proposed to calculate the likelihood (Kingma and Welling 2013) and used for anomaly detection (An and

Cho 2015). To estimate the density more precisely, autoregressive models (Oord, Kalchbrenner, and Kavukcuoglu 2016; Oord et al. 2016) have shown promising results and also been adapted for anomaly detection (Abati et al. 2019). However, these autoregressive models are not efficient for high-dimensional data, cannot be implemented with parallel processing, and are sensitive to the choice of sequence order.

To alleviate these problems, tractable density estimators using normalizing flows have been proposed. NICE (Dinh, Krueger, and Bengio 2014) and Real-NVP (Dinh, Sohl-Dickstein, and Bengio 2016) propose invertible networks using an affine coupling layer and calculate the tractable likelihood using the change of variable theorem. Glow (Kingma and Dhariwal 2018) further improve this using the activation normalization and invertible 1×1 convolution. For video anomaly detection, we are the first to utilize flow-based generative models.

Proposed Method

Overview

In surveillance anomaly detection, normal and anomalous scenes have differences in appearance (e.g., car driving down a sidewalk), motion (e.g., jumping), or both (e.g., chasing a person with an abnormal object). Therefore, representative spatio-temporal feature learning for normal video is important, and we propose a ITAE network that embeds appearance and motion information and a flow-based generative model that estimates each density using these embedding features.

The framework is trained in two steps with only normal training videos. First, in Fig. 2, the sequence of normal video frames are input into the ITAE and pass through the appearance path encoder (E_{app}) and motion path encoder (E_{mot}). The embedding features of the two encoders are combined and reconstructed into original frames through a single decoder. In the second step, with the two embedding features

from the trained ITAE, the normal appearance and motion densities are estimated with flow-based generative models (F_{app} and F_{mot}).

During testing, the abnormality score is calculated using the reconstruction error of the ITAE and the estimated likelihood of the generative model. When an abnormal scene is input, the AE learned with normal frames outputs a high error due to its poor reconstruction. In addition, with generative models, the appearance and motion embedding features obtained from AE are different from the features of the normal training set, which becomes low likelihood value.

Implicit two-path AE

Two-path encoder We design the AE with a two-path encoder to focus on appearance and motion features. The two encoders are specified to embed two different features of a normal scene which are representative information for the input reconstruction. Inspired by SlowFast networks, which show strong performance in action recognition in a simple way without using an optical flow network, we design the two encoders of AE with different input frame rates and a lateral connection between them. Between the frames of the surveillance video, spatial information such as background and pedestrians change very slowly whereas temporal information such as walking or running changes relatively quickly. Therefore, we randomly segment sequential T frames from each clip, input T/τ frames at a τ sampling rate to the appearance encoder, and input T frames to the motion encoder (we use $\tau = 4$ in this paper). For AE to perform the reconstruction task, the appearance encoder is intended to embed spatial semantics with a large channel size but small temporal size of kernels and the motion encoder is intended to embed the normal temporal pattern with the opposite size of kernels (in Table 1). There is a lateral connection that concatenates the appearance path feature with the motion path feature by matching the temporal channel size with a $(5, 1, 1)$ convolutional kernel (the same as in the SlowFast Network). With these two encoders bring a higher reconstruction error than one-path encoder for scenes with abnormal motion or appearance, and perform anomaly detection more effectively (visualized error maps are shown in Fig. 3).

Decoder The two embedding feature maps obtained from each encoder are reconstructed into original input frames through a decoder. In the same way as the lateral connection of each layer between encoders, the two final feature maps are channel-wise concatenated and decoded (shown in Fig. 2). For the decoder to generate the output by grasping the relationships between the appearance and motion features, we do not use the skip connection between the encoder and decoder, which is mainly used in the U-Net AE structure. Without using a complex structure, the ITAE that consists of four layers in each encoder and decoder is more powerful than the other proposed AE, even when using inception blocks or a convLSTM structure with pre-trained network.

Table 1: Instantiation of the ITAE. The numbers in parentheses denote the kernel size (temporal \times spatial) and the output size is in the order of {channel \times temporal \times spatial} size.

Layer	Encoder		Output size
	Appearance	Motion	
Conv1	(1, 3 ²) stride: 1, 2 ²	(5, 3 ²) stride: 1, 2 ²	app: 96 \times 4 \times 128 ² motion: 12 \times 16 \times 128 ²
Conv2	(1, 3 ²) stride: 1, 2 ²	(3, 3 ²) stride: 1, 2 ²	app: 128 \times 4 \times 64 ² motion: 16 \times 16 \times 64 ²
Conv3	(3, 3 ²) stride: 1, 2 ²	(3, 3 ²) stride: 1, 2 ²	app: 256 \times 4 \times 32 ² motion: 32 \times 16 \times 32 ²
Conv4	(3, 3 ²) stride: 1, 1 ²	(3, 3 ²) stride: 1, 1 ²	app: 256 \times 4 \times 32 ² motion: 32 \times 16 \times 32 ²
Layer	Decoder		Output size
DeConv1	(3, 3 ²) stride: 1, 1 ²		256 \times 4 \times 32 ²
DeConv2	(3, 3 ²) stride: 2, 2 ²		128 \times 8 \times 64 ²
DeConv3	(3, 3 ²) stride: 2, 2 ²		96 \times 16 \times 128 ²
DeConv4	(3, 3 ²) stride: 1, 2 ²		3 \times 16 \times 256 ²

Learning normality distribution

We can learn normality from unlabeled normal training data by the unsupervised density estimation method. Using explicit likelihood generative models, it is possible to compute the likelihood of input data. A flow-based generative model can calculate the tractable likelihood via changes of variables toward a simple distribution (e.g. multivariate Gaussian). The likelihood is calculated by passing an invertible parametric function composed of multiple layers that effectively maps the complex data distribution to the simple distribution. Using an input variable $\mathbf{x} \in X$, the distribution of which is unknown, a simple known distribution $\mathbf{z} \sim p_z$ and a parametric function $\mathbf{f}_\theta : X \rightarrow Z$, the integral of probability density function is

$$\int_{\mathbf{z}} p_z(\mathbf{z}) d\mathbf{z} = \int_{\mathbf{x}} p_x(\mathbf{x}) d\mathbf{x} = \int_{\mathbf{x}} p_z(\mathbf{f}_\theta(\mathbf{x})) \left| \det \left(\frac{\partial \mathbf{f}_\theta}{\partial \mathbf{x}} \right) \right| d\mathbf{x} \quad (1)$$

where $\det \left(\frac{\partial \mathbf{f}_\theta}{\partial \mathbf{x}} \right)$ is the Jacobian determinant of function \mathbf{f}_θ under change of variable theorem. When the generative model \mathbf{f} with parameter θ is $\mathbf{f}_\theta = \mathbf{f}_1 \circ \mathbf{f}_2 \circ \dots \circ \mathbf{f}_M$ and $\mathbf{h}_i = \mathbf{f}_i(\mathbf{h}_{i-1})$ where $\mathbf{h}_0 = \mathbf{x}$ and $\mathbf{h}_M = \mathbf{z}$, the probability density function of \mathbf{x} is as follows with Eq. (2).

$$\log p_x(\mathbf{x}) = \log p_z(\mathbf{z}) + \sum_{i=1}^M \log \left| \det \left(\frac{\partial \mathbf{f}_i}{\partial \mathbf{h}_{i-1}} \right) \right| \quad (2)$$

If the density function of the latent variable \mathbf{z} is tractable such as a Gaussian distribution and the Jacobian matrix $\frac{\partial \mathbf{f}_\theta}{\partial \mathbf{x}}$ is triangular, the likelihood of input variable \mathbf{x} can be simply obtained. We use the Glow (Kingma and Dhariwal 2018) model with L level multi-scale architecture and K series of Actnorm, invertible convolution, and Affine layer for density

estimation (please refer to (Kingma and Dhariwal 2018) for more information).

With maximizing the likelihood in Eq. (2), a flow-based generative model estimates the density of high-dimensional data through multiple layers of convolutional network. Since the likelihood of a generative model heavily depends on the image complexity (Serrà et al. 2019), in contrast to Glow, which begins from the image space, the intermediate latent feature of AE is used for effective density modeling. After training the ITAE with frame reconstruction, we estimate the density of the embedding features obtained from each path. The max-pooling and average-pooling along the channel axis of the feature from each path are applied to reduce the dimensions and are concatenated and input into each generative model F_{app} and F_{mot} with multiple layers (shown in Fig. 2). Here, we also concatenate the resized intensity of the input frame or error map of the reconstructed output to the F_{app} input, which gives additional sparse appearance information of the feature map (the ablation studies are conducted with this additional appearance information).

Training and test method

Reconstruction loss function For reconstruction, to make all pixels of the RGB or gray channel similar, the model is trained by minimizing the L2 loss of the input sequence of frames \mathbf{I} that is the ground truth and the output frames $\hat{\mathbf{I}}$ (Eq. (3)).

$$L_2 = \left\| \mathbf{I} - \hat{\mathbf{I}} \right\|_2 \quad (3)$$

In addition, following (Liu et al. 2018), to prevent reconstructing the blurred output due to L2 loss, we add a gradient loss L_{grad} to maintain the sharpness of the input frames. It computes difference of gradient at each pixel between the input and output frames. The reconstruction loss is the sum of L2 and L_{grad} loss in Eq. (4).

$$L_{recon} = L_2 + L_{grad} \quad (4)$$

Log-likelihood loss function After training ITAE, the generative models F_{app} and F_{mot} are trained with the negative log-likelihood (nll) L_{nll} of the appearance and motion embedding feature \mathbf{x}^a and \mathbf{x}^m in Eq. (5). As in Eq. (2), the exact log-likelihood $\log p_x(\mathbf{x}; \theta)$ of the input feature is calculated through flow-based generative models, and the parameters θ are updated to maximize this in Eq. (6).

$$L_{nll} = NLL(\mathbf{x}^a) + NLL(\mathbf{x}^m) \quad (5)$$

$$\begin{aligned} \theta^* &= \arg \max_{\theta} \log p_x(\mathbf{x}; \theta) \\ NLL(\mathbf{x}) &= -\log p_X(\mathbf{x}) \end{aligned} \quad (6)$$

Test method The anomaly score for the reconstruction error $R(\mathbf{I}_t, \hat{\mathbf{I}}_t)$ of the t -th frame is the difference between the T input frames and the output frames of the ITAE (in Eq. (7)). For each frame, we compute the mean of error values in all segments in which it appears. The score $L(\mathbf{x}_t^a, \mathbf{x}_t^m)$ from the generative models is calculated by adding the nll values of

Table 2: Comparison with state-of-the-art methods on three benchmark databases.

Methods		UCSD Ped2	CUHK	ShangHai Tech
non-Reconstruction	MPPCA (Kim and Grauman 2009)	0.693	-	-
	MPPCA+SPA (Mahadevan et al. 2010)	0.613	-	-
	MDT (Mahadevan et al. 2010)	0.829	-	-
	AMDN (Xu et al. 2017)	0.908	-	-
	Unmasking (Tudor Ionescu et al. 2017)	0.822	0.806	-
	MT-FRCN (Hinami, Mei, and Satoh 2017)	0.922	-	-
	Frame-Pred (Liu et al. 2018)	0.954	0.849	0.728
	AMC (Nguyen and Meunier 2019a)	0.962	0.869	-
	Mem-guided (Park, Noh, and Ham 2020)	0.970	0.885	0.705
	Reconstruction	AE-Conv2D (Hasan et al. 2016)	0.850	0.800
AE-Conv3D (Zhao et al. 2017)		0.912	0.771	-
TSC (Luo, Liu, and Gao 2017b)		0.910	0.806	0.679
StackRNN (Luo, Liu, and Gao 2017b)		0.922	0.817	0.680
AbnormalGAN (Ravanbakhsh et al. 2017)		0.935	-	-
HybridAE (Nguyen and Meunier 2019b)		0.922	0.817	0.680
Auto-reg (Abati et al. 2019)		0.954	-	0.725
MemAE (Gong et al. 2019)		0.941	0.833	0.712
Mem-guided (Park, Noh, and Ham 2020)		0.902	0.828	0.698
ITAE (ours)		0.968	0.855	0.718
ITAE + Generative Modeling (ours)		0.973	0.860	0.730

each appearance and the motion feature as a ratio of intervals in Eq. (8).

$$R(\mathbf{I}_t, \hat{\mathbf{I}}_t) = -\log_{10} \left(1 - |\mathbf{I}_t - \hat{\mathbf{I}}_t| \right) \quad (7)$$

$$L(\mathbf{x}_t^a, \mathbf{x}_t^m) = \frac{\lambda_1 NLL(\mathbf{x}_t^a) + \lambda_2 NLL(\mathbf{x}_t^m)}{\lambda_1 + \lambda_2}$$

$$\lambda_1 = \max(\mathbf{x}^a) - \min(\mathbf{x}^a), \lambda_2 = \max(\mathbf{x}^m) - \min(\mathbf{x}^m) \quad (8)$$

The total anomaly score S_t is computed by summing the normalized reconstruction error and nll in Eq. (9).

$$S_t = \text{norm}(R(\mathbf{I}_t, \hat{\mathbf{I}}_t)) + \lambda_L \text{norm}(L(\mathbf{x}_t^a, \mathbf{x}_t^m)) \quad (9)$$

where $\text{norm}(\cdot)$ is normalization within a video clip \mathbf{I} ,

$$\text{norm}(R(\mathbf{I}_t, \hat{\mathbf{I}}_t)) = \frac{R(\mathbf{I}_t, \hat{\mathbf{I}}_t) - \min(R(\mathbf{I}, \hat{\mathbf{I}}))}{\max(R(\mathbf{I}, \hat{\mathbf{I}})) - \min(R(\mathbf{I}, \hat{\mathbf{I}}))}$$

Experiments

Experimental details

Databases We experiment on three real-world scenarios of surveillance video databases and all training set consist only of normal videos and test set includes abnormal scene with frame-level label. (1) The UCSD Ped2 database (Li, Mahadevan, and Vasconcelos 2013) is composed of two overlooking walkway scenes obtained through a mounted camera. Therefore, the foreground object size and movement changes are small and videos are grayscale and low-resolution. There are non-pedestrian objects in the walkways such as cars and skaters in the test set and the density of pedestrians varies. (2) The CUHK Avenue database (Lu, Shi, and Jia 2013) consists of normal video in the training set with a few outliers included and a slight camera shake. The test set includes a person walking in the wrong direction, strange actions, has large motion, and scale of foreground variation. (3) The Shanghai Tech Campus dataset (Liu et al. 2018) (ST) is the largest volume database, containing 13 different scenes. This database includes diverse anomalous events such as brawling and loitering including sudden motion in multiple scenes and is challenging due to its complex angles and lighting conditions.

Table 3: Ablation studies of appearance and motion path in AE and flow-based generative model on three benchmark databases.

Approaches		UCSD Ped2					CUHK					Shanghai Tech				
ITAE	App.	✓	✓	✓	✓	✓	✓	✓	✓	✓	✓	✓	✓	✓	✓	✓
	Motion		✓	✓	✓	✓		✓	✓	✓	✓		✓	✓	✓	✓
Generative modeling	App.			✓		✓			✓		✓			✓		✓
	Motion				✓	✓				✓	✓				✓	✓
AUC		0.959	0.968	0.974	0.973	0.973	0.820	0.855	0.864	0.854	0.860	0.716	0.718	0.725	0.723	0.730

Implementations For training, we resize the input frame to 256×256 and set $T = 16$. We use Adam optimizer (Kingma and Ba 2014) and Cosine annealing scheduler (Loshchilov and Hutter 2016). In first training step, the batch sizes are 2, 4, and 8 and learning rates are $1e^{-3}$, $1e^{-3}$, and $2e^{-4}$ for UCSD, CUHK, and ST database, respectively. For second-step, batch sizes are 20, 32, and 16 and learning rates are $5e^{-4}$, $5e^{-4}$, and $1e^{-4}$. The Glow is used for the flow-based model with $K = 32$ and $L = 3$ ($L = 1$ for UCSD). For UCSD, which have small scale of foregrounds, the original frame size (240×360) is inputted, the latent feature map is reduced to 1/4 times of inputs, and multi-scale SSIM (Wang, Simoncelli, and Bovik 2003) is added to the reconstruction loss. During testing, reconstruction score for UCSD is max of error values within the patch (32×32) of the input frames and for ST, we remove background with MOG-based (Mixture-of-Gaussians) approach following (Abati et al. 2019). Please refer to the supplementary material for detailed information.

Comparison with state-of-the-art methods

For the evaluation, by following comparison works, we compute the average area under curve (AUC) through the receiver operation characteristic (ROC) by gradually changing the threshold of anomaly score in a frame-level annotated database (the ROC curves are reported in the supplementary material). Table 2 shows a comparison between our method and other state-of-the-art methods in the three databases. Among the reconstruction-based methods, our approach shows the best performance in UCSD Ped2, CUHK, and ST, at 97.3%, 86%, and 73%, respectively. These are better results than Auto-reg (Abati et al. 2019), which performs density estimation with an auto-regressive generative model that needs a causal network and data ordering to perform sequential operations.

In non-reconstruction method, good performance is achieved by the Mem-guided (Park, Noh, and Ham 2020), which is a prediction-based method that stores and updates normal query features by memory module. However, this approach shows low performance on ST database with thirteen scenes, which indicates that using memory items may not good enough for complex and multiple scenes. In addition, Frame-Pred (Liu et al. 2018) and AMC (Nguyen and Meunier 2019a) also show high performance, but they are dependent on a pre-trained optical flow network. Our approach shows competitive or better results without using pre-trained network, and ITAE brings large improved performance than well-designed AE (AE-Conv3D (Zhao et al. 2017), TSC (Luo, Liu, and Gao 2017b), and StackRNN (Luo, Liu, and Gao 2017b)).

Table 4: Ablation studies with additional information at appearance generative model.

Database	-	Intensity	Error map
UCSD Ped2	0.973	0.974	0.973
CUHK	0.856	0.864	0.860
Shanghai Tech	0.724	0.725	0.727

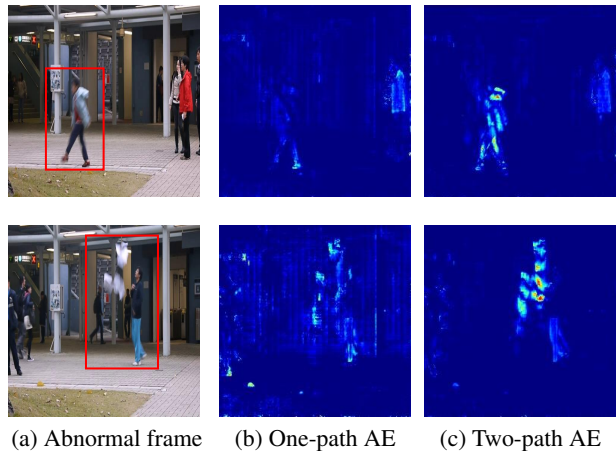


Figure 3: Reconstruction error of one-path AE and two-path AE in abnormal frames.

Discussions

Ablation studies Ablation studies are conducted to show the effectiveness of the ITAE and normality density estimation. In ITAE, the appearance encoder has a sparse temporal rate input and a large channel size of features to focus more on spatial information than motion information, whereas the motion encoder has a high (4 times) temporal rate and small (1/8 times) channel sizes. As shown in Table 3, using the motion path together and passing the concatenate of two encoded features to a decoder performs better in all three databases than using only the appearance path. Among them, in the CUHK database, where there is variation of foreground scale and the motion is large, the greatest performance improvement is achieved at 3.5% when motion path is added.

The performance is boosted with density estimation through both generative models. Since the CUHK database contains some outliers in the training set and there is a slight camera shake, the motion generative model degrades performance with some video clips. In the ST database, which has the largest number of training data and various anomalous

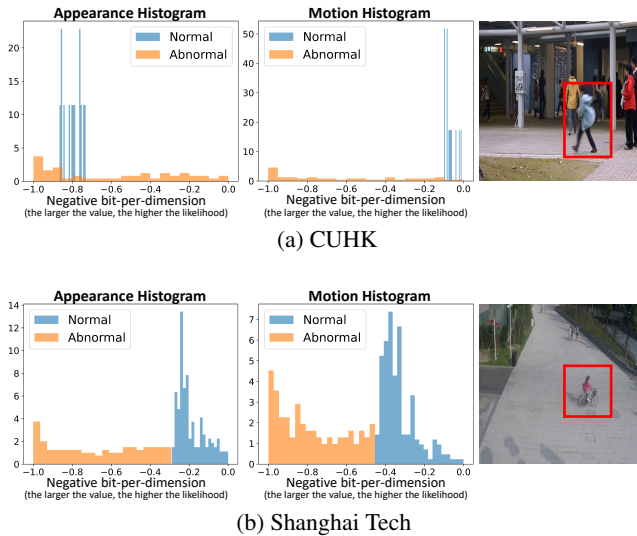


Figure 4: Appearance and motion log-likelihood (expressed in normalized negative bits-per-dimension) histogram within a video clip. (a) Abnormal scene in motion. (b) Abnormal scene in motion and appearance.

events in the test set, the performance increases the most when the flow generative models are added to ITAE, that flow models learn more general normal distribution with a huge amount of training data.

Additional appearance information We conduct an experiment by channel-wise concatenation of the resized frame intensity or error map to give additional spatial information to the appearance generative model. In Table 4, it is better to use additional information and 0.8% performance improved in CUHK. This result shows that although the additional information is sparse, it is helpful to give background or foreground information.

Qualitative results In Fig. 3, we compare output of one-path AE (consisting of only appearance encoder) and ITAE. Following (Park, Noh, and Ham 2020), the error maps are visualized by marking the pixel that is larger than the average error value within the frame. The first row of figure is a jumping kid whose appearance is normal, which leads to low reconstruction error with one-path AE. On the other hand, the ITAE, which focuses on motion as well as appearance, shows a large error due to the poor reconstruction for inputs that are different from the learned normal motion. As for the second row, a person throwing a paper, not only the abnormal of the paper appearance, but also the abnormality of the flying motion leads to a large error in ITAE.

Fig. 4 is a histogram of likelihood within a video clip from appearance and motion flow-based generative models. Fig. 4 (a) is a video clip of a jumping kid among walking pedestrians, and it is difficult to distinguish by the likelihood of the appearance flow model because the normal and abnormal frames look similar. However, since the difference in motion between walking and jumping is large, the histogram of motion flow shows that normal likelihood is low

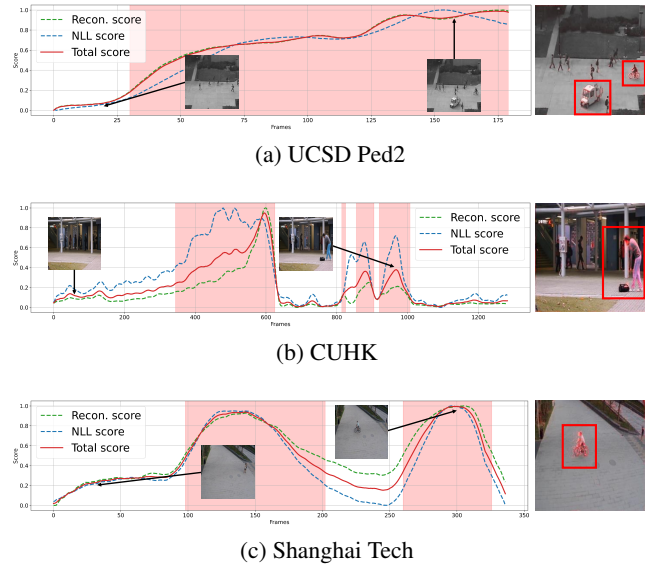


Figure 5: Abnormal scores within a video clip and abnormal frames (reconstruction errors are colored in red) in three benchmark databases. The x-axis is the frame range and the y-axis is a normalized score. The green dashed lines, blue dashed lines, and red lines indicate two-path AE score, generative model score, and total score in Eq. (9). The red highlighted ranges are ground-truth abnormal frames.

in the abnormal frame. In Fig. 4 (b), the likelihoods of both flow models are low for the bike and its speed, which has abnormal appearance and motion on the sidewalk.

With the two-path encoder and their appearance and motion embedding features, we compute the anomaly score of each frame in Fig. 5. By adding the nll score to the reconstruction score, in (b), the total score can better detect anomalies. The two scores complement each other and bring satisfactory results, even when the pedestrian density is high or low and the foreground scale is small or large. Please refer to the supplementary material for various qualitative results.

Conclusion

In this paper, we proposed an ITAE and density estimation of normal features based on a flow-based generative model in an unsupervised manner for video anomaly detection. We designed a ITAE to captures representative spatial and temporal information of normal scenes without using pre-trained network. In addition, with embedding features from ITAE, we modeled the distribution of normal appearance and motion with a flow-based generative model. Through the experiment on standard benchmarks, ITAE showed high effectiveness in scenes where motion is abnormal by learning motion information of normal scenes. Furthermore, the normal distribution modeling of embedded feature leded superior results when the database is large and composed with diverse scenes (in ST database). This can be expected to model general normal distribution and solve practical problems through vast amount of real-world videos with unsupervised learning.

Ethical Impacts CCTVs exist in most places and keep records of our daily lives. This may cause an ethical negative aspect of privacy invasion issues, but since surveillance anomaly detection can quickly cope with crimes and accidents or prevent them in advance, the socially positive impact is much greater. Our work, which is an unsupervised manner, is possible to learn general normal patterns with various scenarios of real-world surveillance video which is promising and expected to accelerate detecting anomalies in our society.

References

- Abati, D.; Porrello, A.; Calderara, S.; and Cucchiara, R. 2019. Latent space autoregression for novelty detection. In *Proceedings of the IEEE Conference on Computer Vision and Pattern Recognition*, 481–490.
- An, J.; and Cho, S. 2015. Variational autoencoder based anomaly detection using reconstruction probability. *Special Lecture on IE 2(1)*: 1–18.
- Bengio, Y.; Lamblin, P.; Popovici, D.; and Larochelle, H. 2007. Greedy layer-wise training of deep networks. In *Advances in neural information processing systems*, 153–160.
- Carreira, J.; and Zisserman, A. 2017. Quo vadis, action recognition? a new model and the kinetics dataset. In *proceedings of the IEEE Conference on Computer Vision and Pattern Recognition*, 6299–6308.
- Chen, D.; Wang, P.; Yue, L.; Zhang, Y.; and Jia, T. 2020. Anomaly detection in surveillance video based on bidirectional prediction. *Image and Vision Computing* 103915.
- Christoph, R.; and Pinz, F. A. 2016. Spatiotemporal residual networks for video action recognition. *Advances in Neural Information Processing Systems* 3468–3476.
- Dinh, L.; Krueger, D.; and Bengio, Y. 2014. Nice: Non-linear independent components estimation. *arXiv preprint arXiv:1410.8516* .
- Dinh, L.; Sohl-Dickstein, J.; and Bengio, S. 2016. Density estimation using real nvp. *arXiv preprint arXiv:1605.08803* .
- Feichtenhofer, C.; Fan, H.; Malik, J.; and He, K. 2019. Slow-fast networks for video recognition. In *Proceedings of the IEEE international conference on computer vision*, 6202–6211.
- Feichtenhofer, C.; Pinz, A.; and Zisserman, A. 2016. Convolutional two-stream network fusion for video action recognition. In *Proceedings of the IEEE conference on computer vision and pattern recognition*, 1933–1941.
- Ganokratanaa, T.; Aramvith, S.; and Sebe, N. 2020. Unsupervised Anomaly Detection and Localization Based on Deep Spatiotemporal Translation Network. *IEEE Access* 8: 50312–50329.
- Gong, D.; Liu, L.; Le, V.; Saha, B.; Mansour, M. R.; Venkatesh, S.; and Hengel, A. v. d. 2019. Memorizing normality to detect anomaly: Memory-augmented deep autoencoder for unsupervised anomaly detection. In *Proceedings of the IEEE International Conference on Computer Vision*, 1705–1714.
- Goodfellow, I. 2016. NIPS 2016 tutorial: Generative adversarial networks. *arXiv preprint arXiv:1701.00160* .
- Goodfellow, I.; Pouget-Abadie, J.; Mirza, M.; Xu, B.; Warde-Farley, D.; Ozair, S.; Courville, A.; and Bengio, Y. 2014. Generative adversarial nets. In *Advances in neural information processing systems*, 2672–2680.
- Hasan, M.; Choi, J.; Neumann, J.; Roy-Chowdhury, A. K.; and Davis, L. S. 2016. Learning temporal regularity in video sequences. In *Proceedings of the IEEE conference on computer vision and pattern recognition*, 733–742.
- Hinami, R.; Mei, T.; and Satoh, S. 2017. Joint detection and recounting of abnormal events by learning deep generic knowledge. In *Proceedings of the IEEE International Conference on Computer Vision*, 3619–3627.
- Ionescu, R. T.; Khan, F. S.; Georgescu, M.-I.; and Shao, L. 2019a. Object-centric auto-encoders and dummy anomalies for abnormal event detection in video. In *Proceedings of the IEEE Conference on Computer Vision and Pattern Recognition*, 7842–7851.
- Ionescu, R. T.; Smeureanu, S.; Popescu, M.; and Alexe, B. 2019b. Detecting abnormal events in video using narrowed normality clusters. In *2019 IEEE Winter Conference on Applications of Computer Vision (WACV)*, 1951–1960. IEEE.
- Kim, J.; and Grauman, K. 2009. Observe locally, infer globally: a space-time MRF for detecting abnormal activities with incremental updates. In *2009 IEEE Conference on Computer Vision and Pattern Recognition*, 2921–2928. IEEE.
- Kingma, D. P.; and Ba, J. 2014. Adam: A method for stochastic optimization. *arXiv preprint arXiv:1412.6980* .
- Kingma, D. P.; and Dhariwal, P. 2018. Glow: Generative flow with invertible 1x1 convolutions. In *Advances in neural information processing systems*, 10215–10224.
- Kingma, D. P.; and Welling, M. 2013. Auto-encoding variational bayes. *arXiv preprint arXiv:1312.6114* .
- Lee, S.; Kim, H. G.; and Ro, Y. M. 2018. STAN: Spatio-temporal adversarial networks for abnormal event detection. In *2018 IEEE International Conference on Acoustics, Speech and Signal Processing (ICASSP)*, 1323–1327. IEEE.
- Lee, S.; Kim, H. G.; and Ro, Y. M. 2019. BMAN: Bidirectional Multi-Scale Aggregation Networks for Abnormal Event Detection. *IEEE Transactions on Image Processing* 29: 2395–2408.
- Li, W.; Mahadevan, V.; and Vasconcelos, N. 2013. Anomaly detection and localization in crowded scenes. *IEEE transactions on pattern analysis and machine intelligence* 36(1): 18–32.
- Liu, W.; Luo, W.; Lian, D.; and Gao, S. 2018. Future frame prediction for anomaly detection—a new baseline. In *Proceedings of the IEEE Conference on Computer Vision and Pattern Recognition*, 6536–6545.

- Loshchilov, I.; and Hutter, F. 2016. Sgdr: Stochastic gradient descent with warm restarts. *arXiv preprint arXiv:1608.03983* .
- Lu, C.; Shi, J.; and Jia, J. 2013. Abnormal event detection at 150 fps in matlab. In *Proceedings of the IEEE international conference on computer vision*, 2720–2727.
- Lu, Y.; Kumar, K. M.; shahabeddin Nabavi, S.; and Wang, Y. 2019. Future Frame Prediction Using Convolutional VRNN for Anomaly Detection. In *2019 16th IEEE International Conference on Advanced Video and Signal Based Surveillance (AVSS)*, 1–8. IEEE.
- Luo, W.; Liu, W.; and Gao, S. 2017a. Remembering history with convolutional lstm for anomaly detection. In *2017 IEEE International Conference on Multimedia and Expo (ICME)*, 439–444. IEEE.
- Luo, W.; Liu, W.; and Gao, S. 2017b. A revisit of sparse coding based anomaly detection in stacked rnn framework. In *Proceedings of the IEEE International Conference on Computer Vision*, 341–349.
- Mahadevan, V.; Li, W.; Bhalodia, V.; and Vasconcelos, N. 2010. Anomaly detection in crowded scenes. In *2010 IEEE Computer Society Conference on Computer Vision and Pattern Recognition*, 1975–1981. IEEE.
- Markovitz, A.; Sharir, G.; Friedman, I.; Zelnik-Manor, L.; and Avidan, S. 2020. Graph Embedded Pose Clustering for Anomaly Detection. In *Proceedings of the IEEE/CVF Conference on Computer Vision and Pattern Recognition*, 10539–10547.
- Nguyen, T.-N.; and Meunier, J. 2019a. Anomaly detection in video sequence with appearance-motion correspondence. In *Proceedings of the IEEE International Conference on Computer Vision*, 1273–1283.
- Nguyen, T. N.; and Meunier, J. 2019b. Hybrid deep network for anomaly detection. *arXiv preprint arXiv:1908.06347* .
- Oord, A. v. d.; Dieleman, S.; Zen, H.; Simonyan, K.; Vinyals, O.; Graves, A.; Kalchbrenner, N.; Senior, A.; and Kavukcuoglu, K. 2016. Wavenet: A generative model for raw audio. *arXiv preprint arXiv:1609.03499* .
- Oord, A. v. d.; Kalchbrenner, N.; and Kavukcuoglu, K. 2016. Pixel recurrent neural networks. *arXiv preprint arXiv:1601.06759* .
- Park, H.; Noh, J.; and Ham, B. 2020. Learning Memory-guided Normality for Anomaly Detection. In *Proceedings of the IEEE/CVF Conference on Computer Vision and Pattern Recognition*, 14372–14381.
- Pimentel, M. A.; Clifton, D. A.; Clifton, L.; and Tarassenko, L. 2014. A review of novelty detection. *Signal Processing* 99: 215–249.
- Ravanbakhsh, M.; Nabi, M.; Sangineto, E.; Marcenaro, L.; Regazzoni, C.; and Sebe, N. 2017. Abnormal event detection in videos using generative adversarial nets. In *2017 IEEE International Conference on Image Processing (ICIP)*, 1577–1581. IEEE.
- Sabokrou, M.; Fayyaz, M.; Fathy, M.; and Klette, R. 2017. Deep-cascade: Cascading 3d deep neural networks for fast anomaly detection and localization in crowded scenes. *IEEE Transactions on Image Processing* 26(4): 1992–2004.
- Sabokrou, M.; Fayyaz, M.; Fathy, M.; Moayed, Z.; and Klette, R. 2018a. Deep-anomaly: Fully convolutional neural network for fast anomaly detection in crowded scenes. *Computer Vision and Image Understanding* 172: 88–97.
- Sabokrou, M.; Khaloeei, M.; Fathy, M.; and Adeli, E. 2018b. Adversarially learned one-class classifier for novelty detection. In *Proceedings of the IEEE Conference on Computer Vision and Pattern Recognition*, 3379–3388.
- Schlegl, T.; Seeböck, P.; Waldstein, S. M.; Schmidt-Erfurth, U.; and Langs, G. 2017. Unsupervised anomaly detection with generative adversarial networks to guide marker discovery. In *International conference on information processing in medical imaging*, 146–157. Springer.
- Serrà, J.; Álvarez, D.; Gómez, V.; Slizovskaia, O.; Núñez, J. F.; and Luque, J. 2019. Input Complexity and Out-of-distribution Detection with Likelihood-based Generative Models. In *International Conference on Learning Representations*.
- Sultani, W.; Chen, C.; and Shah, M. 2018. Real-world anomaly detection in surveillance videos. In *Proceedings of the IEEE Conference on Computer Vision and Pattern Recognition*, 6479–6488.
- Tran, D.; Bourdev, L.; Fergus, R.; Torresani, L.; and Paluri, M. 2015. Learning spatiotemporal features with 3d convolutional networks. In *Proceedings of the IEEE international conference on computer vision*, 4489–4497.
- Tudor Ionescu, R.; Smeureanu, S.; Alexe, B.; and Popescu, M. 2017. Unmasking the abnormal events in video. In *Proceedings of the IEEE International Conference on Computer Vision*, 2895–2903.
- Wang, Z.; Simoncelli, E. P.; and Bovik, A. C. 2003. Multi-scale structural similarity for image quality assessment. In *The Thirty-Seventh Asilomar Conference on Signals, Systems & Computers, 2003*, volume 2, 1398–1402. Ieee.
- Xu, D.; Yan, Y.; Ricci, E.; and Sebe, N. 2017. Detecting anomalous events in videos by learning deep representations of appearance and motion. *Computer Vision and Image Understanding* 156: 117–127.
- Zhao, Y.; Deng, B.; Shen, C.; Liu, Y.; Lu, H.; and Hua, X.-S. 2017. Spatio-temporal autoencoder for video anomaly detection. In *Proceedings of the 25th ACM international conference on Multimedia*, 1933–1941.
- Zhong, J.-X.; Li, N.; Kong, W.; Liu, S.; Li, T. H.; and Li, G. 2019. Graph convolutional label noise cleaner: Train a plug-and-play action classifier for anomaly detection. In *Proceedings of the IEEE Conference on Computer Vision and Pattern Recognition*, 1237–1246.
- Zhu, Y.; and Newsam, S. 2019. Motion-aware feature for improved video anomaly detection. *arXiv preprint arXiv:1907.10211* .